Microsatellite Instability is Present in a Subset of Follicular Thyroid Carcinomas

Research Thesis

Presented in Partial Fulfillment of the Requirements for graduation

with Research Distinction in Molecular Genetics in the undergraduate colleges of

The Ohio State University

By

Luke K. Genutis

The Ohio State University

April 2018

Project Advisor: Dr. Albert de la Chapelle, Department of Molecular Genetics

Table of Contents

ABSTRACT

Microsatellite instability (MSI) is a term used to describe the somatic addition or loss of bases within repetitive DNA sequences called microsatellites and is characteristic of certain cancer types- specifically endometrial cancer (~30% of patients), colorectal cancer (~15% of patients) and stomach cancer (~15% of patients). MSI can have prognostic and predictive implications, and recently MSI was shown to be a predictor of response to anti-Programmed Death Ligand 1 (PD-L1) immunotherapy, which has substantially improved outcome in several cancers. Although the thyroid is one of the most common cancer sites, the prevalence of MSI in thyroid cancer has not been accurately defined. Previous studies on MSI in thyroid cancer have focused almost exclusively on the most common histological subtype, papillary thyroid carcinoma (PTC). Herein we have screened for MSI in a large set of thyroid cancer samples representing all major histologic subtypes.

Defining MSI status has been standardized by polymerase chain reaction (PCR) of five specific microsatellites, and tumors are considered MSI-positive (MSI+) if at least two of the five markers show MSI. Using PCR, we screened a total of 191 thyroid cancer cases including: 122 PTC, 35 follicular thyroid carcinomas (FTC), 20 medullary thyroid carcinomas, and 14 anaplastic thyroid carcinomas. MSI was observed in 5% of FTC cases by PCR and validated with immunohistochemistry staining of the MMR proteins. A separate cohort of 184 thyroid carcinoma cases of various histologies was screen for MSI using a more recent technique based on next-generation sequencing (NGS). A total of 10 cases were predicted to be MSI by this method, three of which were FTCs.

The presence of MSI in FTC, even in a small percentage of cases, could have important clinical implications. Screening for MSI is already performed for newly diagnosed colorectal cancers in Ohio hospitals, as part of the Ohio Colorectal Cancer Prevention Initiative. FTC patients could likewise be screened for MSI upon diagnosis, and patients shown to be MSI positive could be treated with the remarkable PD-1 immunotherapy. Together, this project will provide a comprehensive evaluation of MSI in thyroid cancer.

INTRODUCTION

Microsatellites:

Microsatellites are repetitive DNA sequences of one to five nucleotides that are found throughout the genome. There is no well-accepted rule for when a repeat is considered long enough or short enough to be classified as a microsatellite, rather than a mini or macrosatellite; repeats as short as three units, or as long as several hundred have both been defined as microsatellites[1].

In the human genome, whole genome sequencing (WGS) data has revealed as many as 253,000 microsatellites, and the densities of microsatellites are similar on all chromosomes[2]. Because microsatellites are more susceptible to mutation than non-repetitive DNA sequences, there is selective pressure against microsatellites in exons. In addition, the high mutability of microsatellites means that the length of most microsatellites is highly variable between individuals in the population. This allows microsatellite lengths to serve as a 'DNA fingerprint' to facilitate identifying DNA.

Mismatch Repair (MMR)

Any mechanism involving the synthesis of new DNA may generate changes in length within microsatellites or other repeats, be it from replication, recombination, or repair, however this is usually corrected with mismatch repair[2]. Mismatch repair proteins (MMR) are responsible for correcting base substitution mismatches, as well as single-base insertions or deletions (indels) during DNA replication. MMR also prevents recombination of divergent DNA sequences, which improves genetic stability. MMR can also participate in cell cycle checkpoint control, first by recognizing certain forms of DNA damage, then by triggering a response to this damage such as

cell cycle arrest[3–5]. Recent evidence suggests that deficient MMR leads to a disproportionate increase of single nucleotide variant mutations in genes, rather than nongenic regions of the genome, therefore preferentially protecting genes from mutation[6].

MMR proteins were first discovered in prokaryotes, where loss of expression led to an accumulation of DNA replication errors and a mutator phenotype. MMR begins by recognizing the mismatched base, which can be found structurally due to the resulting distortion of the double helix from the mispairing. MMR must also remove the newly synthesized strand containing the mismatch and allow for it to be resynthesized; strand discrimination between the correct template strand and the incorrect newly synthesized strand is an important feature in MMR systems, although the mechanism for strand discrimination is different in prokaryotes, which recognize $G^{me}ATC$ on the template strand, than in eukaryotes which lack this type of DNA methylation[5].

In *E. coli*, MMR is well understood and is comprised of three proteins: MutS, MutL, and MutH. MutS, an ATPase, binds to the DNA as a homodimer and diffuses along the DNA until it recognizes the mismatch. In this conformation, it is ADP bound. Once bound at the mismatch, ADP is exchanged for ATP, and MutS can move away from the mismatch. MutL, also an ATPase, couples to the activated, mismatch bound MutS. Once MutS becomes ATP bound and can slide away from the lesion, the MutL-MutS complex slides along the DNA until it encounters a methyl bound MutH. MutH is a methylation-sensitive endonuclease that ensures the repair is limited to the newly synthesized DNA strand[5,7–9]. Once a strand break at the methylation site has been generated by MutH, MutS and MutL coordinate recognition of the mismatch site and the break to permit loading of DNA helicase II (UvrD) at the break. DNA helicase II unwinds the DNA, and

the growing single stranded newly synthesized DNA is degraded by exonucleases. DNA Helicase II continues to move towards the mismatch, terminating a variable but short distance past it[10,11]. DNA polymerase III engages with the template strand and conducts repair synthesis, and DNA ligase seals the resulting nick[4].

Eukaryotes possess multiple MSH proteins (MutS homologs; MSH2-6 in humans), as well as MLH proteins (MutL homologues; in humans PMS1, PMS2, MLH1, and MLH3), and the mechanism of repair is similar. Rather than a homodimer of MutS binding to the mismatch, MSH2 and either MSH6 or MSH3 form a dimer (called MutSα with MSH2-MSH6, and MutSβ with MSH2 and MSH3). In the case of the MutL homologs, MLH1 may dimerize with either PMS2, PMS1, or MLH3. Of these three potential MLH1 partners, the MLH1-PMS2 dimer (called MutLα) is the best understood. It is known to possess endonuclease activity and interacts with the MutSα/β complex[12]. Eukaryotes lack MutH homologues, and as such MMR is not methyl-directed as in *E. coli*. Instead, eukaryotic MMR is thought to be nick-directed. In mammals, proliferating cell nuclear antigen (PCNA) is co-immunoprecipitated with MSH2, MLH1, and PMS2, which suggests that PCNA could play an important role in MMR and perhaps strand discrimination[13]. Excision is less well understood in eukaryotes, but is thought to involve Exonuclease 1 (Exo1), Replication Protein-A (RPA), Replication Factor C (RFC), and DNA Polymerase delta (Pol δ)[4,14].

Microsatellite Instability and MMR in Cancer

Microsatellite instability (MSI) was discovered when researchers who were attempting to map a predisposing gene for hereditary nonpolyposis colorectal cancer (HNPCC or Lynch syndrome), a highly heritable form of colorectal cancer, found that tumor samples in up to 73% of HNPCC

patients showed shifts in electrophoretic mobility of the dinucleotide microsatellites used for linkage analysis. The authors suggested that replication errors had occurred in these sequences during tumorigenesis, and the phenotype was later termed microsatellite instability (MSI)[15]. The original HNPCC predisposing gene that the researchers had been mapping was later discovered to be a human homolog of *MutS* (*MSH2*), and was found to have somatic as well as germline mutations in MSI tumor cells[16]. MSI tumors were also found to be hypermutated[17]. MSI was later found in other cancer types, and recent studies indicate that MSI is found in as many as 30% of endometrial cancers, 15% of colorectal cancers, and 15% of stomach cancers[18].

MSI is generally detected by the measurement of polymerase chain reaction (PCR) amplicons spanning the microsatellite itself and comparing the resulting amplicon lengths from the tumor DNA sample to the corresponding normal tissue DNA sample. A panel of five microsatellites, consisting of the mononucleotides BAT25 and BAT26, and the dinucleotides D17S250, D2S123, and D5S346, has been standardized for PCR based detection of MSI. A sample is classified as MSI if two out of five markers demonstrated instability[19,20]. Since MSI is due to loss or near loss of MMR activity, immunohistochemistry (IHC) staining of MMR proteins provides another, more direct detection method. Loss of MSH2 or MLH1 leads to complete loss of MMR. MSH2 is needed to stabilize both MSH6 and MSH3, however loss of either MSH6 or MSH3 alone still confers some MMR activity. Nonsense mutations in *MLH1* show loss of MLH1 as well as PMS2 by IHC[12]. Recent advances in next generation sequencing technologies have allowed for the detection of MSI by examining read lengths of the microsatellites covered in the sequencing panel. Examples of variant caller software used for MSI detection include MSIseq[21], mSINGS[22], MonoSeq[23], MSIsensor[24], and MANTIS[25].

MMR and Targeted Immunotherapy: the PD-1 Blockade

Due to their genetic changes, tumor cells can produce antigens that are presented on the cell surface, which are different from the antigens presented by non-tumor cells. The adaptive immune system possesses anti-tumor activity and can recognize these tumor neo-antigens. However, the amplitude of T cell response can be attenuated by inhibitory signals (immune checkpoints). In a normal cell, these immune checkpoints prevent autoimmunity, and protect the cells from damage when the immune system responds to other infections. In tumors, these immune checkpoints are often upregulated and allow the tumor to evade immune system surveillance. As such, targeting these immune checkpoint receptors or ligands is a promising avenue for anti-cancer therapeutics[26].

One such example of these immune checkpoints is programmed death 1 (PD-1), and its ligands, PD-L1 and PD-L2. In a normal cell, PD-L1 expression limits T cell responses and protects tissues from autoimmunity. In tumors, PD-L1 is highly expressed, and is a common feature of the tumor microenvironment of solid tumors such as breast, lung, colon, ovarian, melanoma, bladder, thyroid, and more. The PD-1 receptor is also often found to be upregulated on tumor infiltrating lymphocytes, further contributing to tumor immunosuppression[26,27]. Pharmacologic inhibition of PD-1/PD-L1 interaction restores T cell activity towards tumor cells. PD-1 immunotherapy was initially tested in a variety of cancers, with good responses found in melanomas, renal-cell carcinomas, and lung tumors. However, out of 33 colorectal cases tested initially, only one patient had a response to the treatment[28,29]. It was later inferred that this patient must have had an MMR deficient colorectal cancer (CRC) after another study found remarkable responses in MMR deficient CRC cases compared to MMR proficient CRCs[30]. PD-1 immunotherapy was expanded

to 12 different cancer types, all with MMR deficiency, and many patients had durable responses, and rapid *in vivo* production of tumor neoantigen-specific T cell clones[31]. Using a murine system of MMR deficient colorectal, breast, and pancreatic tumors, it was demonstrated that MMR deficient tumors had an increased mutational load, dynamic mutational profiles, and continued renewal of tumor neoantigens relative to MMR proficient tumors. This robust study functionally elucidated the correlation between MMR deficiency (MSI), immune surveillance, and therefore response to PD-1 immunotherapy.[32]

MSI and Thyroid Cancer

Thyroid Cancer is the eighth most common malignancy in the United States, accounting for an estimated 56,900 new cases in 2017, as well as 2,000 deaths[33]. Thyroid cancer has several histological subtypes: papillary thyroid carcinoma (PTC, 85% of cases), medullary thyroid carcinoma (MTC; 3-5% of cases), follicular thyroid carcinoma (FTC, 2-5% of cases), and anaplastic thyroid carcinoma (ATC), a rare and more aggressive variant in approximately 1% of cases[34]. PTCs originate from the follicular cells that produce thyroid hormones, and are microscopically characterized by the presence of papillae, while FTCs lack this feature. MTCs originate from C cells, also known as parafollicular cells, responsible for producing the hormone calcitonin[35]. ATCs emerge from the follicular cells either *de novo*, or through accumulation of genetic changes in more common thyroid malignancies, such as from PTC cases[35,36].

Extensive evidence is lacking for the presence of MSI (and underlying mutations in MMR genes) in the thyroid malignancies[18,37]. Previous research has primarily focused on PTC, largely neglecting other subtypes of thyroid cancer, and the largest study investigating MSI in thyroid

cancer to date included only 40 cases. There has been some controversy in the literature regarding the percentage of MSI^+ thyroid cancers, with different studies reporting anywhere from 0%-65% of cases are MSI^+[18,38–42].

In this study, we sought to definitively determine the presence of MSI in thyroid cancer. We used PCR-based methods to screen 191 thyroid cancer cases (122 PTCs, 35 FTCs, 20 MTCs, and 14 ATCs). In MSI+ cases, we validated loss of MMR protein expression using IHC staining of MLH1, MSH2, MSH6, and PMS2. We separately used the MonoSeq[23], variant caller to infer MSI status in an independent cohort of 184 thyroid cancer cases that had been previously sequenced using NGS methods. Together, this represents the most comprehensive evaluation of MSI in thyroid cancer to date.

METHODS

Samples: Individuals were recruited from a multidisciplinary thyroid tumor clinic at Ohio State University Wexner Medical Center (OSUWMC) and all cases were histologically confirmed as either PTC, FTC, MTC or ATC. Recruitment took place in OSUWMC primary care and internal medicine clinics. All patients provided written informed consent, completed a questionnaire that included demographic, medical and family history information, and donated a blood sample. Relevant clinical and pathological data for cases were extracted from the electronic medical record.

The experimental protocols were approved by the Institutional Review Board at the Ohio State University. Experiments were carried out in accordance with the approved guidelines.

DNA Extraction: The DNA samples from primary thyroid tumor tissue were snap frozen in liquid nitrogen after biopsy, digested with proteinase K, and extracted using phenol-chloroform methods. For six ATC cases and 30 FTC cases, DNA was extracted from paraffin cores using phenol-chloroform or the QIAamp DNA FFPE Tissue Kit (Qiagen, Hilden, Germany). In the three cases that lacked adjacent normal thyroid tissue, skeletal muscle tissue was used for two cases and lymph node tissue was used for one case.

MSI PCR testing: We designed marker specific PCR primers for amplification of four microsatellites (BAT25, BAT26, D17S250, and D2S123). A fluorescein amidite (FAM) M13 universal forward primer was used to label PCR-products as previously described[43], with the exception of the BAT25 forward primer, for which we used a locus-specific hexachloro-fluorescein phosphoramidite (HEX) labeled primer. Capillary electrophoresis was performed with

an ABI PRISM® 3730 DNA Analyzer to detect strand-slippage mutations indicative of MSI. Malignant samples were compared with their germ line DNA, a negative experimental control, and three MSI+ colorectal cancer control samples.

IHC Staining: Blocks for two putative MSI+ FTC cases were reviewed and stained with antibodies against MLH1, MSH2, MSH6, and PMS2 using 3,3'-Diaminobenzidine (DAB) and hematoxylin. An MMR proficient FTC case served as a positive control.

NGS Analysis: A total of 184 thyroid cancer cases were selected to be sequenced using the oncomine v3 targeted sequencing panel. Sequencing was performed using a SOLiD sequencer. The resulting NGS data were analyzed using the Monoseq[23] variant caller to infer MSI status.

RESULTS

We determined the MSI status of a sizable cohort of thyroid cancer samples with histologic subtypes representative of a typical patient population (122 PTCs, 35 FTCs, 20 MTCs, and 14 ATCs). The cases were screened with PCR amplicons spanning the microsatellites BAT25, BAT26, D17S250, and D2S123 by comparing microsatellite lengths between the tumors and matched normal DNAs (**Table 1 and Figure 1**). Out of 191 cases screened with this method, two FTC cases (FTC-267 and FTC-727) demonstrated MSI (**Table 2**). We confirmed loss of DNA MMR in these samples by IHC staining for MLH1, MSH2, MSH6, and PMS2. FTC-267 showed a loss of MSH2 and MSH6, and FTC-727 had a loss of MLH1 and PMS2 (**Figure 2**). These results are consistent with the findings that loss of MLH1 expression tends to be found with loss of PMS2, and loss of MSH2 expression is found with loss of MSH6 expression[12,44]. Adequate DNA was available for FTC-267 and allowed us to investigate mutations underlying the MMR defect. FTC-267 was whole-exome sequenced and found to have a hemizygous p.W345* (NM_000251.2:c.1035G>A) nonsense mutation in *MSH2* (**Figure 3**). This mutation would lead to a premature stop codon in the protein sequence, and therefore a truncated and quickly degraded protein. This is consistent with our IHC data for this sample, showing a loss of MSH2 and MSH6 expression.

We next sought to validate our discovery efforts in another cohort using next generation sequencing (NGS) methods (**Figure 4a**). The variant caller MonoSeq[23] was used with a separate cohort of 184 thyroid carcinomas of various histologies (**Figure 4b**) that were previously sequenced for a targeted panel containing 29 microsatellites. We used MonoSeq[23] to assign an MSI likelihood score to each sample, and samples with a score >20 are predicted to be MSI. Out

of 184 thyroid carcinoma cases of mixed histologies, 10 cases were predicted to be MSI (**Figure 4b**). Notably, FTC cases accounted for 30% of the total MSI cases, despite FTC representing 5% of the cohort. Furthermore, one of these cases, NGS 141, had hyper mutability consistent with defective MMR (**Figure 5**).

DISCUSSION AND FUTURE DIRECTIONS

Our results indicate the strongest evidence for MSI in thyroid cancer to date. We believe that because we found he MSI is mainly in FTC cases, it may have been overlooked in previous studies focused on PTC cohorts that report MSI is absent in thyroid cancer[39].

We speculate that previous studies which reported a high incidence of MSI in thyroid cancer were reporting technical false positives. These previous reports varied greatly in the microsatellites chosen, did not use the 'gold standard' Bethesda panel of PCR primers[40–42], and relied on polyacrylamide gels to determine PCR product size, rather than capillary electrophoresis. More recent studies on the prevalence of MSI in thyroid cancer have been conducted using NGS methods. One study looked at PTC cases and found ~2% of cases to be MSI^{+}[18], while another study looked at late stage thyroid carcinomas, a phenotype rare in PTC but common in other histologies, and found the rate of MSI to be as high as 3% [31].

Herein we found MSI to be present in 5% of FTC cases, and absent in all other screened histologies (**Table 1**). We were able to confirm MMR deficiency at the protein level in these cases and showed that the tumor with loss of MSH2 and MSH6 harbored a hemizygous nonsense mutation in *MSH2*. (**Figures 2 and 3**). NGS analysis permitted a way to validate our PCR results using a separate cohort. NGS based detection of MSI is similar to the traditional PCR-based detection, in that MSI is detected by measuring the distribution of different length microsatellites in the reads that span each microsatellite. Ten samples were putatively identified as MSI by the MonoSeq[23] variant caller, and interestingly, one of these cases was a widely invasive FTC, which is consistent with the idea that MMR deficient tumors can evade immune surveillance [31,32,45].

Our results imply that clinical screening of FTC cases for MMR deficiency could uncover some patients who are candidates for MSI-directed immune checkpoint inhibitor therapies. Notably, all Ohio CRC patients are already screened for MSI through the Ohio Colorectal Cancer Prevention Initiative (https://clinicaltrials.gov/ct2/show/NCT01850654), and we argue for extending this screening network to Ohio FTC patients. Future work validating these results in more FTC cases will help to more accurately define the overall prevalence of MSI in FTC.

REFERENCES

1. de la Chapelle, A. & Hampel, H. Clinical relevance of microsatellite instability in colorectal cancer. *J. Clin. Oncol.* **28,** 3380–3387 (2010).
2. Richard, G.-F., Kerrest, A. & Dujon, B. Comparative Genomics and Molecular Dynamics of DNA Repeats in Eukaryotes. *Microbiol. Mol. Biol. Rev.* **72,** 686–727 (2008).
3. Kolodner, R. Biochemistry and genetics of eukaryotic mismatch repair. *Genes Dev* **10,** 1433–1442 (1996).
4. Kunkel, T. A. & Erie, D. A. Dna Mismatch Repair. *Annu. Rev. Biochem.* **74,** 681–710 (2005).
5. Harfe, B. D. & Jinks-Robertson, S. DNA mismatch repair and genetic instability. *Annu. Rev. Genet.* **34,** 359–399 (2000).
6. Belfield, E. J. *et al.* DNA mismatch repair preferentially protects genes from mutation. *Genome Res.* **28,** 66–74 (2018).
7. Modrich, P. & Lahue, R. Mismatch Repair in Replication Fidelity, Genetic Recombination, and Cancer Biology. *Annu. Rev. Biochem.* **65,** 101–133 (1996).
8. Fang, W. H. & Modrich, P. Human strand-specific mismatch repair occurs by a bidirectional mechanism similar to that of the bacterial reaction. *J. Biol. Chem.* **268,** 11838–11844 (1993).
9. Holmes, J., Clark, S. & Modrich, P. Strand-specific mismatch correction in nuclear extracts of human and Drosophila melanogaster cell lines. *Proc. Natl. Acad. Sci. U. S. A.* **87,** 5837–5841 (1990).
10. Viswanathan, M., Burdett, V., Baitinger, C., Modrich, P. & Lovett, S. T. Redundant Exonuclease Involvement in Escherichia coli Methyl-directed Mismatch Repair. *J. Biol.*

Chem. **276,** 31053–31058 (2001).

11. Burdett, V., Baitinger, C., Viswanathan, M., Lovett, S. T. & Modrich, P. In vivo requirement for RecJ, ExoVII, ExoI, and ExoX in methyl-directed mismatch repair. *Proc. Natl. Acad. Sci. U. S. A.* **98,** 6765–70 (2001).
12. Boland, C. R., Koi, M., Chang, D. K. & Carethers, J. M. The biochemical basis of microsatellite instability and abnormal immunohistochemistry and clinical behavior in Lynch Syndrome: from bench to bedside. *Fam. Cancer* **7,** 41–52 (2008).
13. Gu, L., Hong, Y., McCulloch, S., Watanabe, H. & Li, G. M. ATP-dependent interaction of human mismatch repair proteins and dual role of PCNA in mismatch repair. *Nucleic Acids Res.* **26,** 1173–1178 (1998).
14. Fishel, R. Mismatch repair. *J. Biol. Chem.* **290,** 26395–26403 (2015).
15. Aaltonen, L. A. *et al.* Clues to the pathogenesis of familial colorectal cancer. *Science* **260,** 812–6 (1993).
16. Leach, F. S. *et al.* Mutations of a mutS homolog in hereditary nonpolyposis colorectal cancer. *Cell* **75,** 1215–25 (1993).
17. Parsons, R. *et al.* Hypermutability and Mismatch Repair Deficiency in RER+ Tumor-Cells. *Cell* **75,** 1227–1236 (1993).
18. Hause, R. J., Pritchard, C. C., Shendure, J. & Salipante, S. J. Classification and characterization of microsatellite instability across 18 cancer types. *Nat Med* **22,** 1342–1350 (2016).
19. Boland, C. R. *et al.* A National Cancer Institute Workshop on Microsatellite Instability for cancer detection and familial predisposition: development of international criteria for the determination of microsatellite instability in colorectal cancer. *Cancer Res.* **58,** 5248–57

(1998).

20. Umar, A. *et al.* Revised Bethesda Guidelines for hereditary nonpolyposis colorectal cancer (Lynch syndrome) and microsatellite instability. *J. Natl. Cancer Inst.* **96,** 261–8 (2004).
21. Ni Huang, M. *et al.* MSIseq: Software for assessing microsatellite instability from catalogs of somatic mutations. *Sci. Rep.* **5,** 1–10 (2015).
22. Salipante, S. J., Scroggins, S. M., Hampel, H. L., Turner, E. H. & Pritchard, C. C. Microsatellite instability detection by next generation sequencing. *Clin. Chem.* **60,** 1192–1199 (2014).
23. Walker, C. J. *et al.* MonoSeq Variant Caller Reveals Novel Mononucleotide Run Indel Mutations in Tumors with Defective DNA Mismatch Repair. *Hum. Mutat.* **37,** 1004–1012 (2016).
24. Niu, B. *et al.* MSIsensor: Microsatellite instability detection using paired tumor-normal sequence data. *Bioinformatics* **30,** 1015–1016 (2014).
25. Kautto, E. A. *et al.* Performance evaluation for rapid detection of pan-cancer microsatellite instability with MANTIS. *Oncotarget* **8,** 7452–7463 (2017).
26. Pardoll, D. M. The blockade of immune checkpoints in cancer immunotherapy. *Nat. Rev. Cancer* **12,** 252–264 (2012).
27. Keir, M. E., Butte, M. J., Freeman, G. J. & Sharpe, A. H. PD-1 and Its Ligands in Tolerance and Immunity. *Annu. Rev. Immunol.* **26,** 677–704 (2008).
28. Brahmer, J. R. *et al.* Phase I study of single-agent anti-programmed death-1 (MDX-1106) in refractory solid tumors: Safety, clinical activity, pharmacodynamics, and immunologic correlates. *J. Clin. Oncol.* **28,** 3167–3175 (2010).
29. Topalian, S. L. *et al.* Safety, Activity, and Immune Correlates of Anti–PD-1 Antibody in

Cancer. *N. Engl. J. Med.* **366,** 2443–2454 (2012).

30. Le, D. T. *et al.* PD-1 Blockade in Tumors with Mismatch-Repair Deficiency. *N. Engl. J. Med.* **372,** 2509–2520 (2015).
31. Le, D. T. *et al.* Mismatch repair deficiency predicts response of solid tumors to PD-1 blockade. *Science (80-.).* **357,** 409–413 (2017).
32. Germano, G. *et al.* Inactivation of DNA repair triggers neoantigen generation and impairs tumour growth. *Nature* **552,** 116–120 (2017).
33. Siegel, R. L., Miller, K. D. & Jemal, A. Cancer statistics, 2017. *CA. Cancer J. Clin.* **67,** 7–30 (2017).
34. Fagin, J. A. & Wells, S. A. Biologic and Clinical Perspectives on Thyroid Cancer. *N. Engl. J. Med.* **375,** 1054–67 (2016).
35. Carling, T. & Udelsman, R. Thyroid Cancer. *Annu. Rev. Med.* **65,** 125–137 (2014).
36. Bonhomme, B. *et al.* Molecular pathology of anaplastic thyroid carcinomas: a retrospective study of 144 cases. *Thyroid* thy.2016.0254 (2017). doi:10.1089/thy.2016.0254
37. Kim, T. M., Laird, P. W. & Park, P. J. The landscape of microsatellite instability in colorectal and endometrial cancer genomes. *Cell* **155,** 858–868 (2013).
38. Soares, P., Dos Santos, N. R., Seruca, R., Lothe, R. A. & Sobrinho-Simoẽs, M. Benign and malignant thyroid lesions show instability at microsatellite loci. *Eur. J. Cancer* **33,** 293–296 (1997).
39. Bauer, A. J. *et al.* Evaluation of adult papillary thyroid carcinomas by comparative genomic hybridization and microsatellite instability analysis. *Cancer Genet. Cytogenet.* **135,** 182–186 (2002).

40. Mitmaker, E., Alvarado, C., Bégin, L. R. & Trifiro, M. Microsatellite instability in benign and malignant thyroid neoplasms. *J. Surg. Res.* **150,** 40–8 (2008).

41. Onda, M. *et al.* Microsatellite instability in thyroid cancer: Hot spots, clinicopathological implications, and prognostic significance. *Clin. Cancer Res.* **7,** 3444–3449 (2001).

42. Lazzereschi, D. *et al.* Microsatellite instability in thyroid tumours and tumour-like lesions. *Br. J. Cancer* **79,** 340–5 (1999).

43. Schuelke, M. An economic method for the fluorescent labeling of PCR fragments A poor man ' s approach to genotyping for research and high-throughput diagnostics . *Nat. Biotechnol.* **18,** 233–234 (2000).

44. de la Chapelle, A. & Hampel, H. Clinical relevance of microsatellite instability in colorectal cancer. *J. Clin. Oncol.* **28,** 3380–3387 (2010).

45. Bouffet, E. *et al.* Immune checkpoint inhibition for hypermutant glioblastoma multiforme resulting from germline biallelic mismatch repair deficiency. *J. Clin. Oncol.* **34,** 2206–2211 (2016).

ACKNOWLEDGEMENTS

We acknowledge the OSU Department of Pathology, OSU CCC tissue sample bank for their support in tissue acquisition and preparation. We'd like to thank Barbara Fersch, and Jan Lockman for their administrative support. This work was supported by National Cancer Institute Grants P30CA16058 and P50CA168505, and The Ohio State University Pelotonia Undergraduate Fellowship Program.

FIGURES AND TABLES

Table 1. Microsatellite PCR Primers

Primer Name	Primer Sequence (5' to 3')
M13-FAM	TGTAAACGACGGCCAGT
BAT25F-HEX	TCGCTTCCAAGAATGTAAGT
BAT25R	TGTGGATTTTAACTATGGCTC
D2S123F	TGTAAAACGACGGCCAGTAAACAGGATGCCTGCCTTTA
D2S123R	GGACTTTCCACCTATGGGAC
D17S250F	TGTAAAACGACGGCCAGTGGAAGAATCAAATAGACAAT
D17S250R	GCTGGCCATATATATATTTAAACC
BAT26F	TGTAAAACGACGGCCAGTGACTACTTTTGACTTCAG
BAT26R	AACCATTCAACTTTTTAACC

PCR based microsatellite detection was facilitated using an M13 tagged universal primer to permit fluorescent detection with capillary electrophoresis. PCR protocol was according to previous methods[43].

Figure 1. PCR Based Detection of MSI

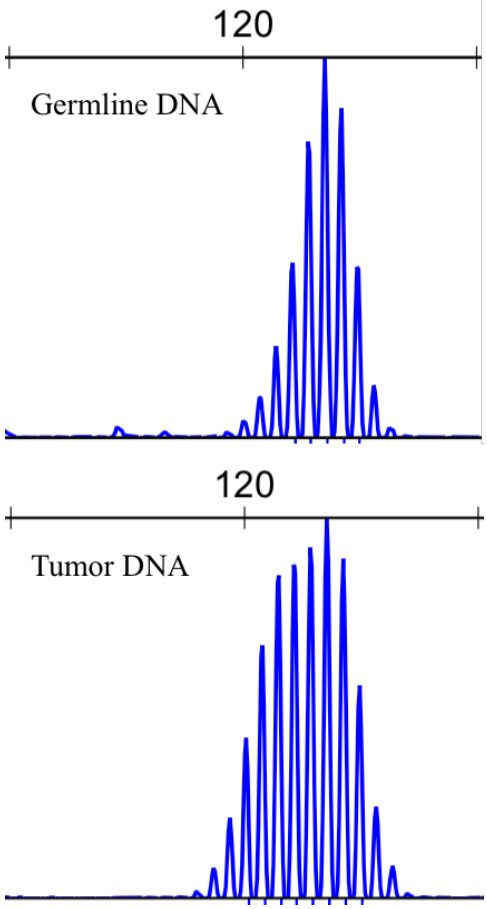

Fig. 1 Electropherograms of Microsatellite PCR markers were compared between tumor DNA and corresponding normal tissue DNA for each case. An example of a strand-slippage mutation in BAT25 is shown. The amplified tumor DNA has additional shorter microsatellites, creating an overall bimodal distribution of amplicon lengths, when compared to the paired germline DNA, indicating MSI.

Table 2. Total Results of the PCR Screen

Histology	Total Cases	Unstable Cases	% Unstable
Anaplastic Thyroid Carcinoma (ATC)	14	0	-
Follicular Thyroid Carcinoma (FTC)	35	2	5.7
Medullary Thyroid Carcinoma (MTC)	20	0	-
Papillary Thyroid Carcinoma (PTC)	122	0	-
Total Cases	191		

Table 2 We screened 191 cases for MSI using the microsatellite markers BAT25, BAT26, D17S250 and D2S123. A total of two FTCs were found to be MSI by this PCR-based detection method, with the case FTC 267 was found to be unstable at BAT25 and D2S123, and FTC 727 was unstable at all four markers tested.

Figure 2. IHC staining of MSI FTCs by PCR

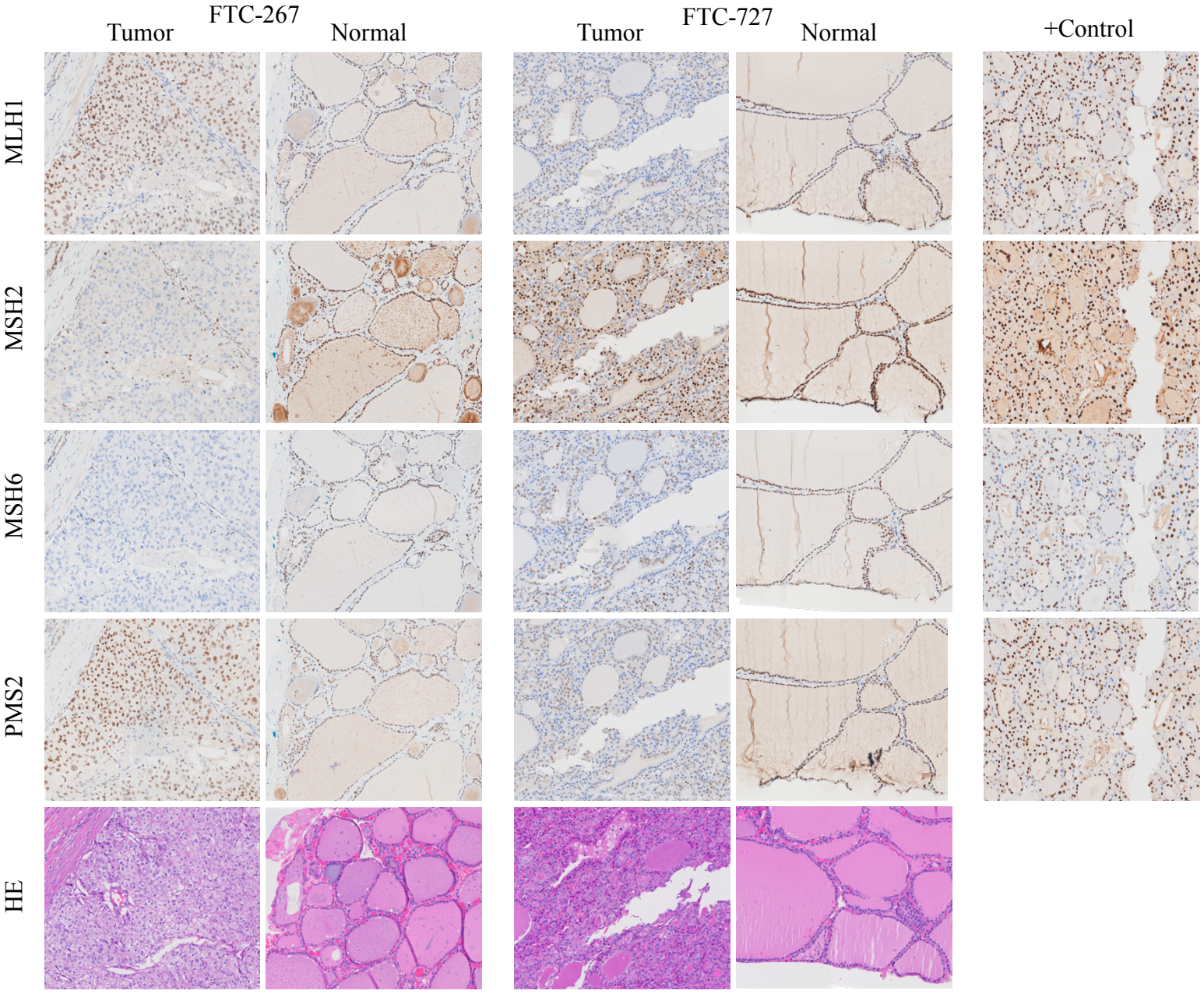

Fig. 2 Immunohistochemistry (IHC) staining of the MMR proteins MLH1, MSH2, MSH6, PMS2, and hemoxylin and eosin (HE). MMR proficient cells for each stain have brown nuclei, while MMR deficient cells have only hematoxylin staining in the nuclei (blue). Sample FTC-267 showed a loss of MSH2 and MSH6, while sample FTC-727 showed a loss of MLH1 and PMS2. An MMR proficient tumor sample serves as the positive control for the MMR protein staining (+Control).

Figure 3. Targeted sequencing validation of underlying MMR mutation.

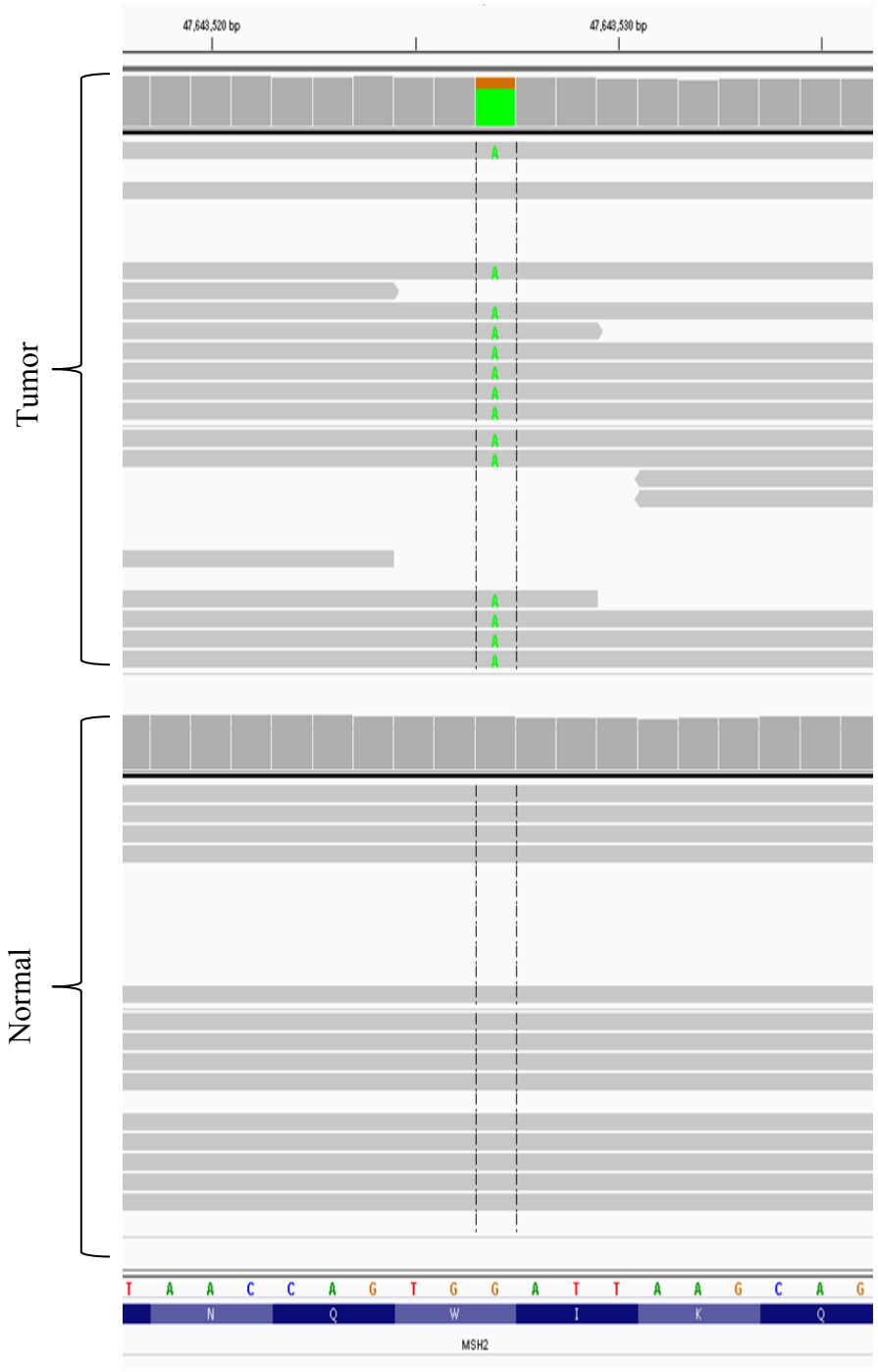

Fig. 3 DNA was available for one of the MSI+ FTCs. Whole exome sequencing was performed and revealed an MSH2 mutation underlying the MSI.

Whole exome sequencing of paired tumor and normal DNA from FTC-267, visualized by integrated genomics viewer. The tumor DNA (top) has a G>A transition that is not evident in the normal DNA (bottom). This transition is a nonsense mutation (p. W345*), and loss-of-heterozygosity can be inferred because the mutation is present in 75% of reads.

Figure 4. NGS based screen of a validation cohort.

A

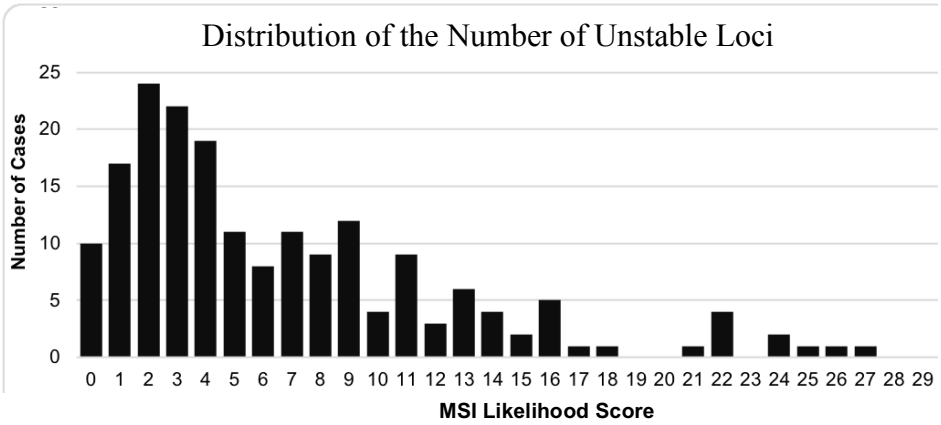

B

Histology	Total cohort	MSI+	% MSI+
FTC	**10**	**3**	**30%**
PTC	73	3	4%
ATC	36	2	6%
MTC	45	1	2%
Hurtle Cell	3	0	0%
Poorly Diff.	17	1	6%
Total	184	10	5%

Fig 4. The MonoSeq variant caller was used to detect MSI in SOLiD sequencing data from 184 thyroid carcinoma cases of various histologies. A. Distribution of MSI likelihood score for all screened cases in this cohort. Cases with scores >20 are predicted to be MSI+. B. Histological subtype distribution shows FTCs are enriched in the MSI+ cases, compared to other histologies.

Figure 5. Mutational profile of the 10 putative MSI cases by NGS

Case	Diagnosis	Mutations
NGS151	ATC	3
NGS 188	ATC	2
NGS 032	FTC-WI	1
NGS 141	FTC-WI	9
NGS 142	FTC-WI	1
NGS 157	MTC	1
NGS 75	PD	2
NGS 13	PTC	2
NGS 101	PTC	1
NGS 185	PTCfv/PD	0

Fig. 5 Mutational landscape of the 10 putative MSI thyroid carcinoma case. 30% of cases are FTC and widely invasive. Of these, NGS-141 is also hypermutated with a mutational load of 9 mutated genes covered by the oncomine panel. ATC= Anaplastic thyroid carcinoma; FTC-WI=follicular thyroid carcinoma, widely invasive; MTC=medullary thyroid carcinoma; PD=poorly differentiated thyroid carcinoma; PTC=papillary thyroid carcinoma; PTCfv=follicular variant.